Inorg. Chem. **1989**, *28*, 1793-1801 **1793**

Contribution from the Department of Chemistry and Biochemistry,
University of Maryland, College Park, Maryland 20742

$FeCl_3$–Phosphine Adducts with Trigonal-Bipyramidal Geometry. Influence of the Phosphine on the Spin State

J. David Walker and Rinaldo Poli*

Received December 6, 1988

Anhydrous FeCl interacts with phosphine ligands in various solvents and in various molar ratios to afford the adducts $FeCl_3(PR_3)_n$ (R = Ph, c-C_6H_{11}, $n = 1, 2$; R = Me, $n = 1$–3). The 1:1 adducts could only be characterized by low-temperature EPR spectroscopy. They are high-spin ($S = {}^5/_2$) mononuclear compounds with a tetrahedral geometry. They decompose in aromatic hydrocarbons and halogenated hydrocarbons by complex pathways, including oxidation of the solvent C–H bonds. The 1:2 adducts were isolated and fully characterized. The PPh_3 and PMe_3 adducts were also characterized crystallographically. $FeCl_3(PPh_3)_2$: orthorhombic, space group *Pbca*, $a = 17.934$ (2) Å, $b = 17.075$ (3) Å, $c = 22.403$ (3) Å, $V = 6860$ (3) Å^3, $Z = 8$, $d_c = 1.33$ g·cm^{-3}, μ(Cu Kα) = 67.90 cm^{-1}, $R = 0.066$, $R_w = 0.066$ for 199 parameters and 1916 observations with $F_o^2 > 3\sigma(F_o^2)$. $FeCl_3(PMe_3)_2$: orthorhombic, space group *Pnma*, $a = 9.846$ (2) Å, $b = 10.680$ (3) Å, $c = 13.439$ (7) Å, $V = 1413$ (1) Å^3, $Z = 4$, $d_c = 1.48$ g·cm^{-3}, μ(Cu Kα) = 156.99 cm^{-1}, $R = 0.053$, $R_w = 0.066$ for 64 parameters and 558 observations with $F_o^2 > 3\sigma(F_o^2)$. Both compounds show a trigonal-bipyramidal structure with the two phosphine ligands in the axial positions. All bond parameters are comparable with the notable exception of the Fe–P bond lengths, which are (average) 2.64 Å in the PPh_3 and 2.335 Å in the PMe_3 derivative. Other properties of these compounds also differ: $FeCl_3(PPh_3)_2$ is a high-spin ($S = {}^5/_2$) compound, as shown by magnetic susceptibility and EPR studies. $FeCl_3(PMe_3)_2$ is EPR silent at liquid-nitrogen temperature and shows a temperature-dependent magnetic moment in solution, consistent with an equilibrium between $S = {}^5/_2$ and $S = {}^3/_2$ spin states, the latter being the ground state. A temperature-independent (in the 10–300 K range) magnetic susceptibility corresponding to three unpaired electrons is observed in the solid state. $FeCl_3(PMe_3)_3$ can only be obtained in equilibrium with the 1:2 adduct in the presence of a large excess of PMe_3. Its EPR spectrum is consistent with a low-spin ($S = {}^1/_2$) state and an octahedral coordination geometry with a meridional configuration. Visible spectroscopic properties and a qualitative MO diagram for these species are also discussed.

Introduction

We are interested in coordinatively unsaturated inorganic and organometallic compounds with an odd number of electrons in the metal valence shell as potential one-electron-transfer agents and were attracted by the Fe(II)/Fe(III) redox couple and by the paucity of iron(III) adducts with phosphine ligands.

Compounds of iron(III) containing soft donor ligands in general are not common. Arsine adducts described as $2FeCl_3·3AsR_3$ and $2FeCl_3·4AsR_3$ (AsR_3 = diphenylmethylarsine, *o*-tolyldimethylarsine) were prepared by Nyholm as early as 1946.[1] Later, Nyholm prepared similar adducts with bidentate arsine ligands, described as $[Fe(diarsine)_2X_2][FeX_4]$ [X = Cl, Br; diarsine = *o*-$C_6H_4(AsMe_2)_2$].[2] The $[FeX_4]^-$ ion can be replaced by other singly charged anions.[2,3]

Analogous derivatives with bidentate phosphines have also been reported.[4] Another class of Fe(III) compounds containing bidentate phosphines, $[Fe(C_5H_5)(dppe)X][PF_6]$ [dppe = bis(diphenylphosphino)ethane; X = monodentate anionic ligand] has been described by Treichel.[5] No structural study appears to have been carried out on these compounds, although $[Fe(diarsine)_2Cl_2][ClO_4]$ has been shown by a powder diffraction study to be isomorphous with the cobalt analogue, which contains the *trans*-$[Co(diarsine)_2Cl_2]^+$ cation.[6]

Iron(III) adducts with *mono*dentate phosphine ligands have been even less studied. Interaction of $Fe_3(CO)_{12}$ with PPh_3 or $AsPh_3$ (L) in $CHCl_3$ yields yellow products formulated as $FeCl_3L$ on the basis of analytical[7] and Mössbauer[8] data. The triphenylphosphine adduct has been later used to catalyze the cross-coupling of alkenyl halides and Grignard reagents.[9] On the other hand, interaction of $FeCl_3$ with PPh_3 or $AsPh_3$ in diethyl ether has been reported to yield 1:2 adducts, for which a dinuclear structure, $[FeCl_3L_2]_2$, has been proposed.[10] This compound catalyzes the oxidation of triphenylphosphine to triphenylphosphine oxide.[11] Again, the structural assignments for these compounds are not supported by crystallographic studies.

We studied the interaction of $FeCl_3$ with monodentate phosphines (PPh_3, PMe_3, PCy_3; Cy = cyclohexyl) in more detail and report here our findings, which comprise the first crystallographic and EPR spectroscopic characterization of this class of derivatives and the first example of an intermediate-spin ($S = {}^3/_2$) Fe(III) compound in a trigonal-bipyramidal geometry.

Experimental Section

All operations were carried out under an atmosphere of dinitrogen by using standard glovebox and Schlenk-tube techniques. Solvents were dried and deoxygenated and distilled under dinitrogen prior to use. Instruments used were as follows: FTIR, Nicolet 5DXC and Perkin-Elmer 1800; EPR, Bruker ER200; NMR, Brucker AF200 and Brucker AM400; magnetic susceptibility balance, Johnson Matthey; UV/vis, Shimadzu UV-240; GC, Hewlett-Packard 5890A. Elemental analyses were by Dr. F. Kasler, Chemistry Department, University of Maryland, by Galbraith Laboratories, Knoxville, TN, and by Midwest Microlab, Indianapolis, IN.

$FeCl_3$ was dehydrated by treatment in $SOCl_2$, and PPh_3 was recrystallized from absolute ethanol. PMe_3 and PCy_3 were purchased from Strem Chemicals. PMe_3 was purified by trap-to-trap distillation, while PCy_3 was used as received.

Preparation of $FeCl_3(PPh_3)_2$. PPh_3 (2.157 g, 8.22 mmol) was added to a suspension of anhydrous $FeCl_3$ (0.667 g, 4.11 mmol) in 20 mL of toluene at −20 °C and the resulting mixture stirred at that temperature for 1 h. The black crystalline product was filtered, washed with 10 mL of toluene, and dried in vacuo; yield 2.34 g (83%). Anal. Calcd for $C_{36}H_{30}Cl_3FeP_2$: C, 63.0; H, 4.4; Cl, 15.5. Found: C, 62.2; H, 4.3; Cl, 16.3. Magnetic susceptibility: $\chi_g = 21.96 \times 10^{-6}$ cgsu; $\mu_{eff} = 6.17\ \mu_B$ (diamagnetic correction $\chi_M = -492.5 \times 10^{-6}$) (lit.[10] $\mu_{eff} = 5.94\ \mu_B$). IR (Nujol mull, cm^{-1}): 1480 m, 1435 s, 1093 m, 742 s, 705 m, 962 s, 512 m, 500 m, 494 m, 372 m. UV/visible [toluene, room temperature, λ/nm (ϵ/L·mol^{-1}·cm^{-1})]: 275 (8000, sh), 285 (12000), 320 (6800, sh), 360 (6200). Single crystals for X-ray analysis were obtained by layering the filtered solution from the reaction with *n*-heptane at −20 °C.

Preparation of $FeCl_3(PMe_3)_2$. PMe_3 (2.0 mL, 20 mmol) was added to a suspension of anhydrous $FeCl_3$ (1.63 g, 10.1 mmol) in 25 mL of toluene at room temperature and the resulting mixture stirred for 1 h. The purple crystalline product was filtered, washed with 20 mL of tolu-

---

[1] Nyholm, R. S. *J. Proc. R. Soc. N.S.W.* **1946**, *78*, 229.

[2] (a) Nyholm, R. S. *J. Chem. Soc.* **1950**, 851. (b) Lewis, J.; Nyholm, R. S.; Rodley, G. A. *J. Chem. Soc.* **1965**, 1483. (c) Hazeldean, G. S. F.; Nyholm, R. S.; Parish, R. V. *J. Chem. Soc. A* **1966**, 162.

[3] (a) Silverthorn, W.; Feltham, R. D. *Inorg. Chem.* **1967**, *6*, 1662. (b) Feltham, R. D.; Silverthorn, W.; Wickman, H.; Wesolowski, W. *Inorg. Chem.* **1972**, *11*, 676.

[4] Warren, L. F.; Bennet, M. A. *J. Am. Chem. Soc.* **1974**, *96*, 3340.

[5] (a) Treichel, P. M.; Wagner, K. P.; Mueh, H. J. *J. Organomet. Chem.* **1975**, *86*, C13. (b) Treichel, P. M.; Molzahn, D. C.; Wagner, K. P. *J. Organomet. Chem.* **1979**, *174*, 191.

[6] Pauling, P. J.; Porter, D. W.; Robertson, G. B. *J. Chem. Soc.* **1970**, 2728.

[7] Singh, P. P.; Rivest, R. *Can. J. Chem.* **1968**, *46*, 1773.

[8] Birchall, T. *Can. J. Chem.* **1969**, *47*, 1351.

[9] Neumann, S. M.; Kochi, J. K. *J. Org. Chem.* **1975**, *40*, 599.

[10] Naldini, L. *Gazz. Chim. Ital.* **1960**, *90*, 1231.

[11] Ondrejkovicova, I.; Vancova, V.; Ondrejovic, G. *Collect. Czech. Chem. Commun.* **1983**, *48*, 254.

0020-1669/89/1328-1793$01.50/0

Table I. Crystal Data for $FeCl_3L_2$ Compounds (L = PPh_3, PMe_3)

compd	$FeCl_3(PPh_3)_2$	$FeCl_3(PMe_3)_2$
formula	$C_{36}H_{30}Cl_3FeP_2$	$C_6H_{18}Cl_3FeP_2$
fw	686.79	314.36
space group	*Pbca*	*Pnma*
a, Å	17.934 (2)	9.846 (2)
b, Å	17.075 (3)	10.680 (3)
c, Å	22.403 (3)	13.439 (7)
α, deg	90	90
β, deg	90	90
γ, deg	90	90
V, $Å^3$	6860 (3)	1413 (1)
Z	8	4
d_c, g/cm^3	1.33	1.48
μ(Cu Kα), cm^{-1}	67.90	156.99
radiation (monochromated in incident beam)	Cu Kα (λ = 1.541 78 Å)	Cu Kα (λ = 1.541 78 Å)
temp, °C	20	20
transmissn factors: max, min	1.0000, 0.5872	1.000, 0.511
R^a	0.066	0.053
$R_w{}^b$	0.066	0.066

$^a R = \sum||F_o| - |F_c||/\sum|F_o|$. $^b R_w = [\sum w(|F_o| - |F_c|)^2/\sum w|F_o|^2]^{1/2}$; $w = 1/\sigma^2(|F_o|)$.

ene, and dried in vacuo; yield 2.216 g (70%). Analytically pure product was obtained by carrying out the reaction at −20 °C and layering the filtrate with *n*-heptane and storing at −20 °C. This procedure also gave suitable single crystals for the X-ray analysis. IR (Nujol mull, cm^{-1}): 1405 m, 1300 w, 1285 m, 955 m, 935 s, 850 w, 750 m, 670 w, 335 m, 300 w, 265 w, 250 m. UV/visible [toluene, room temperature, λ/nm (ϵ/L·mol^{-1}·cm^{-1})]: 240 (32 800), 270 (18 400, sh), 285 (10 200, sh), 330 (2800, sh), 378 (3400), 500 (10 000), 575 (2800, sh).

Preparation of $FeCl_3(PCy_3)_2$. PCy_3 (1.33 g, 4.73 mmol) and anhydrous $FeCl_3$ (0.38 g, 2.37 mmol) were reacted in toluene (25 mL) and stirred for $^1/_2$ h at room temperature. A dark brown solution and a brown precipitate were formed. The solid was filtered out and dried under vacuum (336 mg). Treatment of the solution with *n*-heptane (5 mL) and cooling to −20 °C caused the formation of more brown crystalline solid. After the solution was decanted, the product was washed with *n*-heptane and dried under vacuum; yield 565 mg (33%). A satisfactory elemental analysis (C, H) was obtained. IR (Nujol mull, cm^{-1}): 1605 w, 1595 m, 1450 s, 1175 m, 1000 m, 885 m, 850 m, 725 s, 695 m, 465 m. UV/visible [toluene, room temperature, λ/nm (ϵ/L·mol^{-1}·cm^{-1})]: 290 (2600).

X-ray Crystallography. a. $FeCl_3(PPh_3)_2$. A single crystal was introduced under degassed and dry mineral oil in a thin-walled glass capillary, which was then sealed with epoxy resin and mounted on the diffractometer. The preliminary operations and collection of intensity data were routine. Crystal data are assembled in Table I. No decay of intensity was observed in three periodically monitored standard reflections. The space group was uniquely determined from the systematic absences from the data and further confirmed by the successful refinement of the structure. The data were corrected for Lorentz and polarization factors and for absorption.[12] The metal atom and the coordination sphere were obtained by direct methods, and the rest of the structure was obtained and refined by alternate full-matrix least-squares cycles and difference Fourier maps with the TEXSAN package of programs. Hydrogen atoms were included at calculated positions and used for structure factor calculations but not refined. At the end of the isotropic refinement, an additional absorption correction[13] was applied. In order to avoid instability in the refinement, only the iron, chlorine, and phosphorus atoms were refined anisotropically. Atomic coordinates are listed in Table II, and selected bond distances and angles are in Table IV.

b. $FeCl_3(PMe_3)_2$. A single crystal was introduced under degassed and dry mineral oil in a thin-walled glass capillary, which was then sealed with epoxy resin and mounted on the diffractometer. It was analyzed in the same way as the compound $FeCl_3(PPh_3)_2$ described above (crystal data in Table I). Systematic absences from the data indicated that the space group was either *Pnma* or $Pn2_1a$. An *N*(*Z*) test suggested a centric structure, and the *Pnma* space group was selected and later proved to be correct by the successful refinement. Solution and refinement of the structure were conducted in the same way as described above for $FeCl_3(PPh_3)_2$. Hydrogen atoms were introduced at calculated positions but not refined. All the non-hydrogen atoms were refined anisotropically. Final atomic positional and equivalent isotropic thermal parameters are listed in Table III, whereas selected bond distances and angles are in Table V.

Results and Discussion

a. Synthesis and Magnetic and EPR Studies. 1. $FeCl_3(PPh_3)_2$. Anhydrous $FeCl_3$ and PPh_3 interact very rapidly in a variety of solvents, including aromatic hydrocarbons (toluene, benzene) and chlorinated hydrocarbons (CCl_4, $CHCl_3$, CH_2Cl_2) to afford extremely dark solutions. When the interaction is carried out in a 1:2 molar ratio, the resulting solution is stable for variable periods of time, depending on temperature and solvent nature. The decomposition is retarded by the presence of an excess of the phosphine ligand. The decomposition pathways of these solutions are described in more detail later.

When a solution obtained by interacting $FeCl_3$ and PPh_3 in a 1:2 ratio in either CCl_4 or toluene was rapidly worked up at low temperature, a black crystalline material analyzing correctly for $FeCl_3(PPh_3)_2$ was obtained in good yield. Its room-temperature magnetic moment corresponds to 5 unpaired electrons per metal center. This compound seems in all respects identical with that obtained[10] from the same precursors in ether. The IR spectrum shows only one Fe–Cl stretching vibration at 372 cm^{-1}. This does not appear to agree with the earlier formulation of the compound[10] as a chloride-bridged dimer. A crystal structure determination (vide infra) shows that the compound has a trigonal-bipyramidal geometry with the three chloro ligand in equatorial positions. The observed D_{3h} symmetry is in accord with the observed unique Fe–Cl stretching vibration (E′ type).

We wondered whether we could reproduce the known[7] $FeCl_3(PPh_3)$ compound by simple interaction of $FeCl_3$ with PPh_3 in a 1:1 molar ratio. When we carried out this interaction in toluene, $CHCl_3$, or CCl_4, we obtained dark solutions similar to those arising from the 1:2 interaction described above. These solutions decompose in a similar way and at an even faster rate than the corresponding ones with a 1:2 ratio of $FeCl_3$ and PPh_3. Upon cold temperature workup, only small amounts of the black crystalline $FeCl_3(PPh_3)_2$ compound were obtained.

We were puzzled by the difference in color and stability between our 1:1 $FeCl_3/PPh_3$ solutions and the reported yellow[7] $FeCl_3(PPh_3)$, which had been obtained by refluxing $Fe_3(CO)_{12}$ and PPh_3 in $CHCl_3$ and final ethanol workup of the product. We have not been able to prepare this yellow "$FeCl_3(PPh_3)$" by interaction of anhydrous $FeCl_3$ and PPh_3 in equimolar amounts in anhydrous ethanol. The interaction does produce yellow solutions, but the only product that we were able to obtain upon cooling was white crystalline PPh_3.

In order to gain a better understanding of the $FeCl_3$–PPh_3 interaction, we carried out an EPR spectroscopic study of solutions obtained from $FeCl_3$ and variable amounts of PPh_3. The mixtures were prepared at −20 °C and, after brief stirring, transferred into the EPR tube, which was then immediately cooled to the liquid-nitrogen temperature. The decomposition reactions (described in the next section) are believed to be negligible in these conditions.

A representative set of the obtained spectra is shown in Figure 1. When the interaction is carried out in a 1:1 $FeCl_3$:PPh_3 ratio, spectrum a is obtained. This shows as the main feature of a broad and isotropic signal at $g_{eff} = 1.897$, whereas other minor signals can be observed at higher *g* values. Upon addition of phosphine, the signal at $g = 1.897$ decreases in intensity and shifts to higher *g* values, whereas the other signals become more intense. For a 1:2 $FeCl_3$:PPh_3 ratio, the spectrum shown in Figure 1b is obtained. Spectrum c is obtained with a 35:1 phosphine:iron ratio and compares with the spectrum obtained by redissolving pure, crystalline $FeCl_3(PPh_3)_2$ in the same solvent. The signal in the $g = 2$ region is still present, but it is no longer symmetric and its value has shifted to $g_{eff} = 1.952$.

These spectra suggest the following. The strong signal at $g = 1.897$ in spectrum a is probably due to a 1:1 adduct. This has presumably a tetrahedral geometry, which is typical of 4-coordinate Fe(III) complexes. The appearance of this as an isotropic signal suggests that the PPh_3 and the chloro ligands have a similar

---

[12] North, A. C. T.; Phillips, D. C.; Mathews, F. S. *Acta Crystallogr., Sect. A* **1968**, *A24*, 351.

[13] Walker, N.; Stuart, D. *Acta Crystallogr., Sect. A* **1983**, *A39*, 158.

Table II. Positional Parameters and *B*(eq) Values for $FeCl_3(PPh_3)_2$[a,b]

atom	*x*	*y*	*z*	*B*(eq), Å^2
Fe	0.5959 (1)	0.1697 (1)	0.14535 (8)	2.83 (9)
Cl(1)	0.7059 (2)	0.1372 (2)	0.1077 (1)	4.3 (2)
Cl(2)	0.4936 (2)	0.1019 (2)	0.1272 (1)	4.6 (2)
Cl(3)	0.5889 (2)	0.2745 (2)	0.2018 (1)	4.5 (2)
P(1)	0.5638 (2)	0.2496 (2)	0.0470 (1)	2.9 (2)
P(2)	0.6167 (2)	0.0759 (2)	0.2365 (1)	2.8 (2)
C(10)	0.5833 (6)	0.1971 (7)	−0.0214 (5)	3.2 (3)
C(11)	0.5823 (8)	0.116 (1)	−0.0205 (7)	6.2 (4)
C(12)	0.599 (1)	0.071 (1)	−0.0727 (8)	8.0 (5)
C(13)	0.6187 (8)	0.110 (1)	−0.1229 (7)	6.9 (4)
C(14)	0.6193 (8)	0.187 (1)	−0.1247 (7)	6.9 (4)
C(15)	0.6045 (7)	0.2329 (8)	−0.0738 (6)	4.9 (3)
C(20)	0.6087 (6)	0.3443 (7)	0.0373 (5)	2.5 (2)
C(21)	0.6779 (6)	0.3553 (7)	0.0634 (5)	3.3 (3)
C(22)	0.7151 (7)	0.4269 (8)	0.0577 (5)	3.9 (3)
C(23)	0.6829 (7)	0.4857 (8)	0.0234 (6)	4.3 (3)
C(24)	0.6145 (7)	0.4741 (8)	−0.0028 (6)	4.7 (3)
C(25)	0.5771 (6)	0.4043 (8)	0.0038 (5)	3.7 (3)
C(30)	0.4648 (6)	0.2758 (7)	0.0433 (5)	3.2 (3)
C(31)	0.4360 (7)	0.3193 (8)	0.0894 (5)	4.1 (3)
C(32)	0.3581 (9)	0.340 (1)	0.0885 (7)	6.6 (4)
C(33)	0.3181 (8)	0.315 (1)	0.0424 (7)	6.1 (4)
C(34)	0.3434 (8)	0.270 (1)	−0.0017 (7)	6.2 (4)
C(35)	0.4193 (7)	0.248 (1)	−0.0027 (6)	5.7 (3)
C(40)	0.6879 (6)	0.1055 (7)	0.2887 (5)	2.9 (3)
C(41)	0.6853 (7)	0.0920 (8)	0.3488 (6)	4.4 (3)
C(42)	0.7433 (8)	0.1122 (8)	0.3861 (6)	5.4 (4)
C(43)	0.8048 (7)	0.1453 (8)	0.3647 (6)	5.2 (3)
C(44)	0.8113 (8)	0.1585 (9)	0.3066 (7)	5.8 (4)
C(45)	0.7520 (8)	0.1392 (8)	0.2676 (6)	5.4 (3)
C(50)	0.5336 (6)	0.0674 (8)	0.2816 (5)	3.2 (3)
C(51)	0.4998 (8)	−0.003 (1)	0.2941 (6)	5.6 (4)
C(52)	0.432 (1)	−0.005 (1)	0.3270 (7)	7.7 (5)
C(53)	0.4050 (8)	0.065 (1)	0.3490 (7)	6.1 (4)
C(54)	0.4396 (9)	0.133 (1)	0.3405 (7)	6.7 (4)
C(55)	0.5032 (7)	0.1351 (8)	0.3049 (6)	5.0 (3)
C(60)	0.6418 (6)	−0.0221 (7)	0.2159 (5)	2.8 (3)
C(61)	0.7034 (7)	−0.0602 (9)	0.2380 (6)	5.4 (4)
C(62)	0.7195 (8)	−0.136 (1)	0.2209 (7)	6.6 (4)
C(63)	0.6770 (9)	−0.177 (1)	0.1821 (7)	6.2 (4)
C(64)	0.6147 (9)	−0.141 (1)	0.1608 (7)	6.8 (4)
C(65)	0.5978 (8)	−0.064 (1)	0.1774 (6)	5.7 (4)
H(11)	0.5671	0.0893	0.0165	7.2
H(12)	0.6008	0.0126	−0.0704	8.4
H(13)	0.6279	0.0823	−0.1589	6.9
H(14)	0.6347	0.2176	−0.1607	7.1
H(15)	0.6062	0.2911	−0.0748	5.4
H(21)	0.6996	0.3144	0.0884	3.8
H(22)	0.7649	0.4326	0.0736	5.0
H(23)	0.7090	0.5358	0.0190	5.3
H(24)	0.5914	0.5139	−0.0280	5.8
H(25)	0.5270	0.3989	−0.0133	4.0
H(31)	0.4703	0.3359	0.1207	4.8
H(32)	0.3350	0.3708	0.1214	7.3
H(33)	0.2653	0.3300	0.0432	7.0
H(34)	0.3077	0.2589	−0.0343	7.3
H(35)	0.4389	0.2067	−0.0327	6.9
H(41)	0.6391	0.0663	0.3654	4.9
H(42)	0.7383	0.0994	0.4297	7.0
H(43)	0.8462	0.1603	0.3905	6.0
H(44)	0.8534	0.1897	0.2914	6.3
H(45)	0.7578	0.1475	0.2233	6.1
H(51)	0.5198	−0.0500	0.2749	6.6
H(52)	0.4094	−0.0564	0.3401	9.5
H(53)	0.3589	0.0648	0.3733	7.3
H(54)	0.4209	0.1841	0.3581	7.5
H(55)	0.5289	0.1836	0.2967	5.5
H(61)	0.7382	−0.0332	0.2677	6.3
H(62)	0.7656	−0.1609	0.2362	7.4
H(63)	0.6901	−0.2302	0.1727	7.5
H(64)	0.5837	−0.1702	0.1301	8.3
H(65)	0.5497	−0.0428	0.1620	6.8

[a] Numbers in parentheses are estimated standard deviations in the least significant digit. [b] All carbon atoms were refined isotropically. Anisotropically refined atoms are given in the form of the equivalent isotropic displacement parameter defined as $^4/_3[a^2\beta_{11} + b^2\beta_{22} + c^2\beta_{33} + ab(\cos\gamma)\beta_{12} + ac(\cos\beta)\beta_{13} + bc(\cos\alpha)\beta_{23}]$.

Table III. Positional Parameters and *B*(eq) Values for $FeCl_3(PMe_3)_2$[a,b]

atom	*x*	*y*	*z*	*B*(eq), Å^2
Fe	0.7155 (3)	$^1/_4$	0.0203 (2)	2.6 (1)
Cl(1)	0.7904 (3)	0.0738 (3)	0.0906 (2)	4.1 (1)
Cl(2)	0.5722 (5)	$^1/_4$	−0.1084 (3)	4.8 (2)
P(1)	0.8953 (5)	$^1/_4$	−0.0937 (3)	3.5 (2)
P(2)	0.5268 (4)	$^1/_4$	0.1252 (3)	3.0 (2)
C(1)	1.060 (2)	$^1/_4$	−0.037 (1)	5 (1)
C(2)	0.893 (1)	0.3865 (8)	−0.1733 (9)	3.9 (6)
C(3)	0.575 (2)	$^1/_4$	0.255 (1)	5 (1)
C(4)	0.418 (1)	0.1132 (8)	0.108 (1)	4.2 (6)
H(1)	1.0712	0.1886	0.0020	5.5
H(2)	1.1274	$^1/_4$	−0.0884	5.5
H(4)	0.9135	0.4591	−0.1378	4.7
H(5)	0.9685	0.3761	−0.2235	4.7
H(6)	0.8131	0.3923	−0.2092	4.7
H(7)	0.6206	0.1775	0.2675	6.3
H(9)	0.4883	$^1/_4$	0.2910	6.3
H(10)	0.3401	0.1209	0.1477	5.0
H(11)	0.3930	0.1075	0.0395	5.0
H(12)	0.4676	0.0401	0.1258	5.0

[a] Numbers in parentheses are estimated standard deviations in the least significant digit. [b] Anisotropically refined atoms are given in the form of the equivalent isotropic displacement parameter defined as $^4/_3[\alpha^2\beta_{11} + b^2\beta_{22} + c^2\beta_{33} + ab(\cos\gamma)\beta_{12} + ac(\cos\beta)\beta_{13} + bc(\cos\alpha)\beta_{23}]$.

Table IV. Selected Bond Distances (Å) and Angles (deg) and Estimated Standard Deviations for $FeCl_3(PPh_3)_2$

Distances			
Fe–Cl(1)	2.217 (3)	P(1)–C(20)	1.82 (1)
Fe–Cl(2)	2.206 (4)	P(1)–C(30)	1.83 (1)
Fe–Cl(3)	2.194 (4)	P(2)–C(40)	1.80 (1)
Fe–P(1)	2.654 (4)	P(2)–C(50)	1.81 (1)
Fe–P(2)	2.623 (4)	P(2)–C(60)	1.79 (1)
P(1)–C(10)	1.81 (1)		
Angles			
Cl(1)–Fe–Cl(2)	122.6 (2)	Fe–P(1)–C(20)	117.4 (4)
Cl(1)–Fe–Cl(3)	118.3 (1)	Fe–P(1)–C(30)	111.9 (4)
Cl(1)–Fe–P(1)	90.3 (1)	C(10)–P(1)–C(20)	104.7 (5)
Cl(1)–Fe–P(2)	90.9 (1)	C(10)–P(1)–C(30)	105.6 (5)
Cl(2)–Fe–Cl(3)	119.1 (2)	C(20)–P(1)–C(30)	101.9 (5)
Cl(2)–Fe–P(1)	86.4 (1)	Fe–P(2)–C(40)	115.8 (4)
Cl(2)–Fe–P(2)	86.6 (1)	Fe–P(2)–C(50)	111.6 (4)
Cl(3)–Fe–P(1)	92.7 (1)	Fe–P(2)–C(60)	113.9 (4)
Cl(3)–Fe–P(2)	93.3 (1)	C(40)–P(2)–C(50)	104.1 (5)
P(1)–Fe–P(2)	172.4 (1)	C(40)–P(2)–C(60)	104.5 (5)
Fe–P(1)–C(10)	114.0 (4)	C(50)–P(2)–C(60)	106.0 (6)

electronic effect on the iron(III) center, therefore generating an effective cubic symmetry. Spectrum c can be attributed to the mononuclear 1:2 adduct, $FeCl_3(PPh_3)_2$. It exhibits a signal at $g = 5.623$, typical of the perpendicular component in a tetragonal high-spin Fe(III). For a pure axial symmetry ($E = 0$) and a D value much greater than the microwave quantum, signals with $g_\perp = 6$ and $g_\parallel = 2$ are expected.[14] We do not observe a signal a $g \approx 2$ that can be attributed to a parallel component, but this probably overlaps with the stronger signal at $g_{eff} = 1.952$. It is known that when the zero-field-splitting constant D has a value comparable to that of the microwave quantum, more complicated spectra are observed. We believe this to be the case for $FeCl_3(PPh_3)_2$. Considering the axial symmetry of this compound (see the crystallographic study below), we can assume that E will be

---

(14) König, E. In *The Organic Chemistry of Iron*; Koerner von Gustorf, E. A., Grevels, F.-W., Fischler, I., Eds.; Academic Press: New York, 1978; pp 257–299.

Table V. Selected Bond Distances (Å) and Angles (deg) and Estimated Standard Deviations for $FeCl_3(PMe_3)_2$

	Distances		
Fe-Cl(1)	2.231 (3)	P(1)-C(1)	1.79 (2)
Fe-Cl(2)	2.232 (5)	P(1)-C(2)	1.81 (1)
Fe-P(1)	2.342 (5)	P(2)-C(3)	1.81 (2)
Fe-P(2)	2.332 (5)	P(2)-C(4)	1.83 (1)
	Angles		
Cl(1)-Fe-Cl(1)	115.1 (2)	P(1)-Fe-P(2)	176.3 (2)
Cl(1)-Fe-Cl(2)	122.46 (9)	Fe-P(1)-C(1)	114.1 (6)
Cl(1)-Fe-P(1)	91.5 (1)	Fe-P(1)-C(2)	112.2 (4)
Cl(1)-Fe-P(2)	90.4 (1)	Fe-P(2)-C(3)	111.9 (6)
Cl(2)-Fe-P(1)	88.3 (2)	Fe-P(2)-C(4)	113.1 (4)
Cl(2)-Fe-P(2)	88.0 (2)		

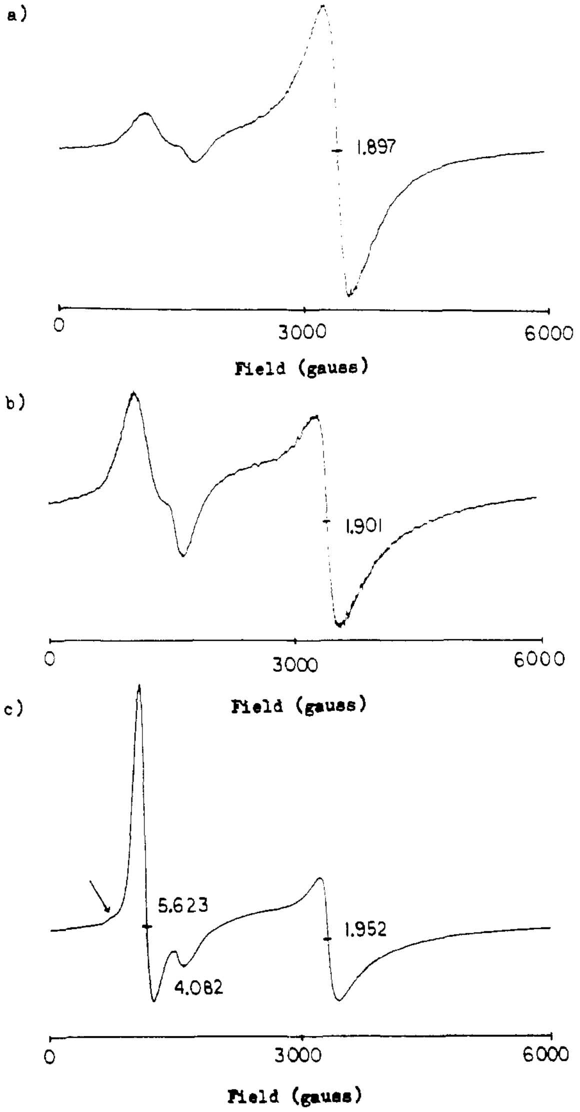

Figure 1. EPR spectra of solutions obtained by interacting $FeCl_3$ and PPh_3 in CH_2Cl_2 at −20 °C. The solution was transferred in the quartz tube shortly after mixing and promptly cooled to 77 K. PPh_3:$FeCl_3$ ratio: (a) 1; (b) 2; (c) 35.

close to 0. According to Dowsing and Gibson,[15] five transitions should be observed for small D; the $^1/_2 \rightarrow -^1/_2$ transition should be nearly isotropic, but the other four (two at higher field, two at lower) should be anisotropic with observable perpendicular and parallel components. Since we do not observe signals at $g < 1.95$ (up to a magnetic field of 12 000 G), an examination of Figure 1 of Dowsing and Gibson[15] suggests a D value larger than 0.2 cm^{-1} for $FeCl_3(PPh_3)_2$. We observe signals at g = 5.623, 4.082, and 1.952, plus a shoulder on the low-field side of the major signal (arrow in Figure 1c). The exact assignment of these bands is not possible in the absence of a single-crystal EPR facility. We cannot exclude that a small amount of the 1:1 adduct remains in equilibrium with $FeCl_3(PPh_3)_2$, even with a 1:35 $FeCl_3$:PPh_3 molar ratio.

The EPR studies described above suggest that reactions 1a and 1b are taking place. A 1:1 mixture of $FeCl_3(PPh_3)_2$ and $FeCl_3$ did not reproduce the EPR spectrum shown in Figure 1a.

$$FeCl_3 + PPh_3 \rightarrow FeCl_3(PPh_3) \tag{1a}$$

$$FeCl_3(PPh_3) + PPh_3 \rightarrow FeCl_3(PPh_3)_2 \tag{1b}$$

In conclusion, the neutral tetrahedral $FeCl_3(PPh_3)$ is an elusive species that can be identified by EPR spectroscopy in toluene at low temperature. It rapidly decomposes at room temperature. We do not know the relationship between this reactive 1:1 adduct and the reported[7] yellow $FeCl_3(PPh_3)$. The latter has been characterized by elemental analysis[7] and Mössbauer spectroscopy.[8] We advance the hypothesis that this yellow product has an ionic formulation (see also the decomposition reactions discussed in the next section). Most of the known derivatives of Fe(III) with soft donor ligands and also a few with hard donor ligands are ionic. Examples are $[Fe(L\text{-}L)_2X_2][FeX_4]$ [X = Cl or Br, L-L = o-$C_6H_4(AsMe_2)_2$;[2] X = Cl, L-L = methylenebis(diphenylphosphine oxide) or tetramethylenebis(diphenylphosphine oxide)[16]] and $[FeCl_2L_4][FeCl_4]$ (L = N-methylimidazole,[17] pyridine N-oxide,[18] dimethyl sulfoxide[19]). Unfortunately, all of these materials correspond to the empirical formula $FeCl_3L_2$ or $FeCl_3(L\text{-}L)$. No ionic compound with an empirical formula $FeCl_3L$, that is with structure $[FeCl_2L_2][FeCl_4]$, seems to have been positively characterized. Four-coordinate tetrahedral Fe(III) is common in anionic species, such as $[FeX_4]^-$ (X = Cl, Br, SR[20]), and has been suggested for the neutral $FeCl_3(THF)$ compound[21] but to the best of our knowledge, is never found in cationic complexes.

2. $FeCl_3(PMe_3)_2$. This compound was prepared in a manner identical with that for its PPh_3 counterpart. The interaction of $FeCl_3$ and 2 equiv of PMe_3 is instantaneous in toluene at room temperature, with production of dark violet solutions. Although the product can be recovered in high yields from these solutions by precipitation with heptane, competing decomposition reactions with formation of white precipitates strongly affect the purity of the compound. The decomposition reaction is retarded by the presence of an excess of the PMe_3 ligand. An analytically pure sample can be obtained, although in smaller yields, by low-temperature workup. The solid product is stable at room temperature under an inert atmosphere.

Compound $FeCl_3(PMe_3)_2$ differs from $FeCl_3(PPh_3)_2$ in several ways. The different color is related to different visible spectroscopic properties, to be discussed in more detail later. Solutions of the PMe_3 adduct, either prepared in situ by the $FeCl_3$–PMe_3 interaction in a 1:2 molar ratio or obtained by redissolving the isolated product, are EPR silent at 77 K. Furthermore, a room-temperature magnetic susceptibility measurement shows a reduced magnetic moment with respect to the pure high-spin ($S = {}^5/_2$) configuration. The effective magnetic moment was found to be 4.22 μ_B in the solid state (average of three measurements with a standard deviation of 0.14) and 4.94 μ_B in solution of aromatic solvents by the Evans method[22] (average of three measurements, σ = 0.23). We initially considered that these observations could be explained by a dinuclear, chloride-bridged structure, which had

---

(15) Dowsing, R. D.; Gibson, J. F. *J. Chem. Phys.* **1969**, *50*, 294.

(16) (a) Lobana, S.; Cheema, H. S.; Sandhu, S. S. *Transition Met. Chem.* (*Weinheim, Ger.*) **1984**, *9*, 119. (b) Lobana, S.; Cheema, H. S.; Sandhu, S. S. *J. Chem. Soc., Dalton Trans.* **1983**, 2039.

(17) Cotton, S. A.; Pisani, P. V. H.; Stubbs, R. *Inorg. Nucl. Chem. Lett.* **1976**, *12*, 695.

(18) Cotton, S. A.; Gibson, J. F. *J. Chem. Soc., Dalton Trans.* **1970**, 2105.

(19) Bennett, M. A.; Cotton, F. A.; Weaver, D. L. *Acta Crystallogr.* **1967**, *23*, 581.

(20) (a) Lippard, S. J. *Acc. Chem. Res.* **1973**, *6*, 282. (b) Holm, R. H. *Acc. Chem. Res.* **1977**, *10*, 427. (c) Koch, S. A.; Maelia, L. E.; Millar, M. *J. Am. Chem. Soc.* **1983**, *105*, 5944. (d) Millar, M.; Lee, J. F.; Koch, S. A.; Fikar, R. *Inorg. Chem.* **1982**, *21*, 4106.

(21) Brenner, L. S.; Root, C. A. *Inorg. Chem.* **1972**, *11*, 652.

(22) Evans, D. F.; James, T. A. *J. Chem. Soc., Dalton Trans.* **1979**, 723.

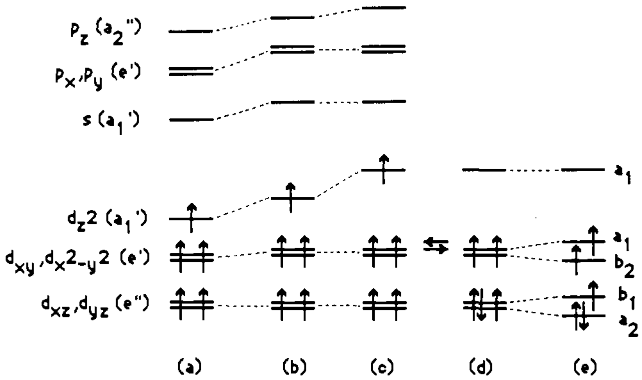

Figure 2. Qualitative molecular orbital diagram for a trigonal-bipyramidal $FeCl_3L_2$ molecule. (a) crystal field splitting; (b) L = PPh_3; (c) L = PMe_3 (high spin); (d) L = PMe_3 (low spin); (e) same L as for (d) plus Jahn–Teller distortion to C_{2v} symmetry.

in fact been proposed earlier[10] for $FeCl_3(PPh_3)_2$. A crystallographic study, however, shows (vide infra) that $FeCl_3(PMe_3)_2$, like $FeCl_3(PPh_3)_2$, is a mononuclear, trigonal-bipyramidal compound.

The qualitative molecular orbital diagram shown in Figure 2 can be easily constructed.[23] Column a shows the energy levels expected on the basis of a pure crystal field perturbation. In columns b and c the effect of the covalent bonding is included. Neither the chloride ions nor the phosphine ligands are expected to add a significant π contribution to the bonding with Fe(III). We shall therefore consider only the ligand orbitals than can be used for σ type combinations. These are of type a_1' and e' for the three chloride ions and of type a_1' and a_2'' for the phosphine ligands. As a result of covalent interactions, both the metal e' (d_{xy}, $d_{x^2-y^2}$) and a_1' (d_{z^2}) orbitals are raised in energy, whereas the e'' (d_{xz}, d_{yz}) orbitals remain unchanged (no ligand-based e'' orbitals are available in a pure σ scheme). The e' orbital is raised only by interaction with the chloride ions, whereas the energy of the a_1' orbital is expected to be raised by interaction with both the chloride ions and (mainly) the phosphine ligands. Consequently, the better σ donor PMe_3 is expected to raise the energy of the a_1' (d_{z^2}) orbital to a higher energy with respect of PPh_3, whereas no effect is expected on the e' levels by a change in phosphine nature (cf. columns b and c in Figure 2).

The experimental room-temperature magnetic data show that in the PPh_3 case the splitting of the d orbitals is not sufficient to cause spin pairing. However, the reduced magnetic moment in the PMe_3 case suggests that there might be a thermal equilibrium between the $^6A_1'$ state and a $S = {}^3/_2$ system obtained by pairing up the fifth electron in the e'' orbitals, that is a $^4E''$ state (this is represented by the equilibrium c $\rightleftarrows$ d in Figure 2). An alternative explanation is that, instead of two discrete spin states $S = {}^5/_2$ and $S = {}^3/_2$ in thermal equilibrium with each other, the system experiences a quantum-mechanical spin-mixing resulting in a single, temperature-dependent, spin-mixed state.[24] Examples of Fe(III) compounds with a ($S = {}^3/_2/S = {}^5/_2$) spin-admixed state have been found.[25] These, however, have a square-pyramidal rather than trigonal-bipyramidal geometry.

We have carried out a variable temperature magnetic susceptibility study in the solid state. The magnetic susceptibility follows the Curie law in the entire range studied (10–300 K), corresponding to an effective magnetic moment of 4.2 μ_B. This value is very close to that expected for three unpaired electrons. A variable-temperature magnetic study has also been carried out in solution by the NMR method.[22] Our temperature range was severely limited by the thermal decomposition of the compound above room temperature and by solvent freezing at low temperatures. We were able, however, to investigate the temperature range 233–296 K and found that the effective magnetic moment drops toward the value observed in the solid state as temperature decreases (see Figure 3). Obviously, this result is relevant from the qualitative point of view only, since no correction for the solvent susceptibility and density at the different temperatures was made.[22]

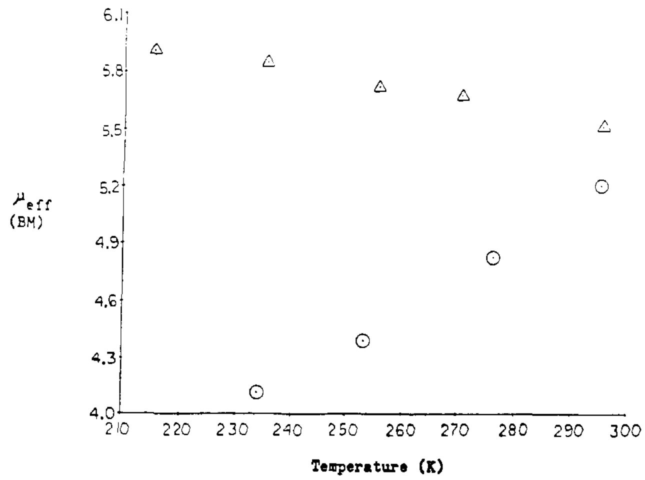

Figure 3. Temperature dependence of the effective magnetic moment for $FeCl_3(PR_3)_2$ (R = Me, Cy): ○, Me; △, Cy. Measurements were done by NMR spectroscopy in toluene-d_8. No correction for the diamagnetic contribution or for the solution density change with temperature was applied.

We conclude that $FeCl_3(PMe_3)_2$, unlike its PPh_3 analogue, is not in a high-spin state. Qualitative molecular orbital considerations, outlined above, allow us to predict that the stronger covalent bonding of PMe_3 may cause spin pairing to a $S = {}^3/_2$ configuration, and the observed magnetic behavior agrees well with this view. The extensive population of the $S = {}^3/_2$ spin state helps rationalize the structural and optical properties of this compound, to be discussed below.

One further question to be addressed is why compound $FeCl_3(PMe_3)_2$ is EPR silent. Considering the magnetic studies discussed above, we would expect that the compound will almost completely populate the $S = {}^3/_2$ ground state at 77 K. Other Fe(III) compounds in an intermediate ($S = {}^3/_2$) spin state have been characterized previously by EPR spectroscopy.[26] One possible explanation is that a fast ($k > 10^{10}$ s^{-1}) spin relaxation mechanism, with consequent broadening of the line, is operating. An alternative explanation is that at low temperature a dimerization process takes place to produce antiferromagnetically coupled iron centers. The dimerization would involve expansion of the coordination number from 5 to 6, which is in fact an observed occurrence when an excess of PMe_3 is added (vide infra). We are planning to investigate this point in more detail at a later date.

Solutions obtained by interacting $FeCl_3$ and PMe_3 in stoichiometric ratios either lower or higher than 1:2, unlike solutions of $FeCl_3(PMe_3)_2$, are EPR active. Representative spectra are reported in Figure 4. The product of the 1:1 interaction (Figure 4a) shows features at $g_{eff} = 5.204$ and at $g_{eff} = 1.940$. This spectrum is similar to that of compound $FeCl_3(PPh_3)_2$ (Figure 1c) and typical of a high-spin ($S = {}^5/_2$) Fe(III) complex with tetragonal symmetry. Our conclusion is that the 4-coordinate, presumably pseudotetrahedral $FeCl_3(PMe_3)$ has been formed. The difference between this spectrum and that attributed to $FeCl_3(PPh_3)$ (shown in Figure 1a) may be due to the stronger field of the PMe_3 ligand, which presumably causes a departure of the **g** tensor from cubic to tetragonal symmetry.

---

(23) (a) Sacconi, L. *Pure Appl. Chem.* **1968**, *17*, 95. (b) Rossi, A. R.; Hoffmann, R. *Inorg. Chem.* **1975**, *14*, 365, and ref 9 therein. (c) Albright, T. A.; Burdett, J. K.; Whangbo, M.-H. *Orbitals Interactions in Chemistry*; Wiley: New York, 1985.

(24) Maltempo, M. M. *J. Chem. Phys.* **1974**, *7*, 2540.

(25) Mitra, S.; Marathe, V. R.; Birdy, R. *Chem. Phys. Lett.* **1983**, *96*, 103, and references therein.

(26) (a) Epstein, I. M.; Straub, D. K.; Maricondi, C. *Inorg. Chem.* **1967**, *6*, 1720. (b) Ogoshi, H.; Sugimoto, H.; Watanabe, E.; Yoshida, Z.; Maeda, Y.; Sakai, H. *Bull. Chem. Soc. Jpn.* **1981**, *54*, 3414. (c) Mansuy, D.; Morgenstern-Badarau, I.; Lange, M.; Gans, P. *Inorg. Chem.* **1982**, *21*, 1427. (d) Maltempo, M. M. *Chem. Phys. Lett.* **1979**, *60*, 441.

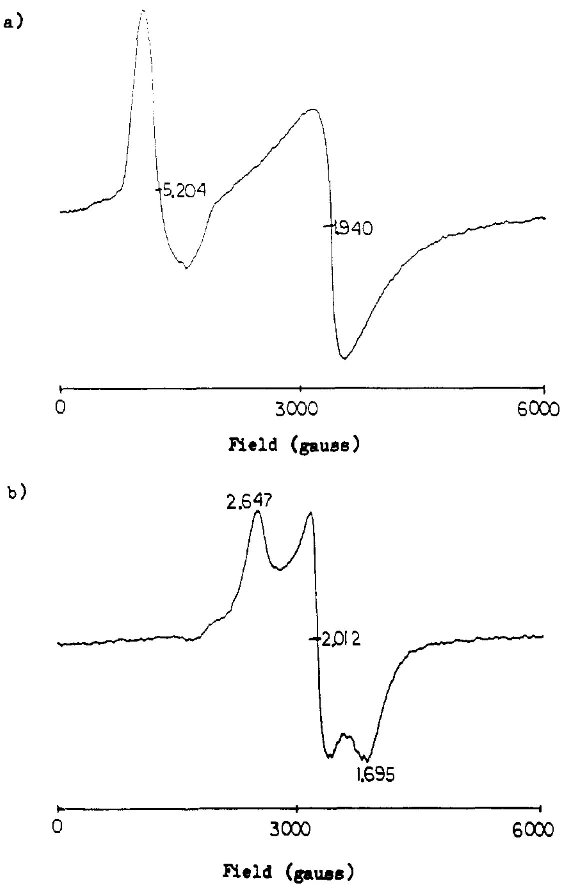

Figure 4. EPR spectra of solutions obtained by interacting $FeCl_3$ and PMe_3 in toluene at 77 K. PMe_3:$FeCl_3$ ratio: (a) 1; (b) 10.

When the $FeCl_3$–PMe_3 interaction is carried out in a 1:10 ratio, the spectrum reported in Figure 4b is obtained. This shows an asymmetric g tensor with the three principal values being 2.647, 2.012, and 1.695. This is a typical spectrum for a low-spin ($S = {}^1/_2$) Fe(III) center.[14] We suggest that an equilibrium exists between the 1:2 adduct of trigonal-bipyramidal geometry and a 1:3 adduct of psuedooctahedral geometry, probably in the meridional configuration. A facial isomer would be expected to display a tetragonal spectrum. Furthermore, octahedral complexes of stoichiometry MX_3L_3 (X = halogen, L = neutral monodentate ligand, M = any transition metal) are known to be more stable in the meridional geometry.[27]

The overall chemical reactivity of the $FeCl_3/PMe_3$ system may be represented by eq 2a–c.

$$FeCl_3 + PMe_3 \rightarrow FeCl_3(PMe_3) \qquad (2a)$$

$$FeCl_3(PMe_3) + PMe_3 \rightarrow FeCl_3(PMe_3)_2 \qquad (2b)$$

$$FeCl_3(PMe_3)_2 + PMe_3 \rightleftarrows FeCl_3(PMe_3)_3 \qquad (2c)$$

Reaction 2b is probably irreversible, since no $FeCl_3(PMe_3)$ is detected by EPR spectroscopy in a 1:2 $FeCl_3/PMe_3$ mixture. On the other hand, equilibrium 2c must be substantially shifted toward the left, since the optical spectrum of a 1:10 $FeCl_3/PMe_3$ solution is identical with that of the same mixture in a 1:2 ratio.

3. $FeCl_3(PCy_3)_2$. The interaction of $FeCl_3$ with tricyclohexylphosphine in a 1:2 ratio led to the formation of the $FeCl_3(PCy_3)_2$ compound. Although we have not yet been able to find suitable single crystals for an X-ray structural analysis on this species, the EPR and magnetic properties point toward a mononuclear trigonal-bipyranidal structure of the same type observed for the PPh_3 and PMe_3 analogues. This compound, like $FeCl_3(PMe_3)_2$, shows a reduced room-temperature magnetic moment ($\mu_{eff} = 5.52\ \mu_B$) with respect to that expected for a pure high-spin configuration. In this case, however, the magnetic moment *increases* with a decrease of temperature (see Figure 3). Its value at 215 K (5.91 μ_B) is in agreement with the spin-only value expected for a $S = {}^5/_2$ state. This shows that the same spin equilibrium between $S = {}^5/_2$ and $S = {}^3/_2$ states already observed for $FeCl_3(PMe_3)_2$ (vide supra) exists in this species, except that in this case *the ground state is the high-spin state*. These observations allow us to assess the phosphine ligand field strength for this type of compound in the order $PPh_3 < PCy_3 < PMe_3$.

Compound $FeCl_3(PCy_3)_2$ exhibits an EPR spectrum at liquid-nitrogen temperature similar to that observed for the PPh_3 analogue, supporting the idea that the two compounds have the same structure.

b. Decomposition Reactions. 1. In Aromatic Hydrocarbons. When toluene solutions of $FeCl_3(PPh_3)_2$ are left standing at room temperature for long periods of time, they deposit a white precipitate and a yellow oily material, while the color of the solution turns to pale yellow. The white material is only sparingly soluble in warm toluene or $CHCl_3$ and decomposes in THF. Its white color suggests that this is a product or mixture of products of iron in the II+ oxidation state. Elemental analyses on this material, however, gave unreproducible results.

In the course of one crystallization of $FeCl_3(PPh_3)_2$, carried out in toluene at −20 °C, a few yellow crystals mixed with the black crystals of the Fe(III) complex were also noted. One of these was investigated crystallographically and found to be of $[PHPh_3][FeCl_4]$.[28] The appearance of a proton in this triphenylphosphonium salt suggests that a solvent C–H bond activation may have taken place. This is subtantiated by a gas-chromatographic analysis of the solution, which revealed the presence of chloro-substituted toluenes. These three observations (formation of Fe(II) products, formation of the $PHPh_3$ salt, and formation of chlorinated toluene) are consistent with eq 3 as a possible decomposition pathway.

$$3FeCl_3(PPh_3) + C_7H_8 \rightarrow 2[FeCl_2(PPh_3)]_x + C_7H_7Cl + PHPh_3[FeCl_4] \qquad (3)$$

This result is particularly significant when compared with the reported[29] chlorination of toluene or benzene by anhydrous $FeCl_3$ to produce, in addition to a mixture of monochlorotoluenes or -benzenes, $FeCl_2$ and HCl. An obvious difference between the chlorination with $FeCl_3$ and the one with $FeCl_3(PPh_3)_x$ is that in the latter cases the phosphine ligand will be able to trap the HCl that is evolved, to form $[PHPh_3]^+$ cations. The observed $[PHPh_3][FeCl_4]$ product formally derives from the interaction of HCl and $FeCl_3(PPh_3)$. We found by gas-chromatographic monitoring of the chlorotoluenes formed that the decomposition reaction is suppressed by an excess of the phosphine ligand. Two factors may be involved in this trend: a lower activity of the iron center when more phosphine ligands are coordinated to it and a "mass effect" of the phosphine ligand reacting with the metal complex as in reaction 1b, assuming that this is an equilibrium reaction. Although $FeCl_3(PPh_3)_2$ might not interact with the aromatic solvent directly and its activity may simply be caused by phosphine dissociation to generate the more reactive $FeCl_3(PPh_3)$ species, further dissociation to the even more reactive $FeCl_3$ seems improbable.

The amount of chlorotoluene generated in the decomposition reaction of $FeCl_3(PPh_3)_x$ in toluene is less than expected on the basis of eq 1. The rest of the Fe(III) material must change its

---

(27) Owens, B. E.; Poli, R.; Rheingold, A. L. *Inorg. Chem.* **1989**, *28*, 1456.

(28) $[PHPh_3][FeCl_4]$. Crystal data: monoclinic, space group $P2_1/n$; a = 17.569 (2) Å; b = 9.938 (1) Å; c = 24.053 (1) Å; β = 97.006 (6)°; V = 4168 (1) Å^3; Z = 8; d_c = 1.47 g·cm^{-3}; μ(Cu Kα) = 113.22 cm^{-1}; R = 0.057; R_w = 0.063 for 433 variables and 3061 observations having $F_o^2 > 3\sigma(F_o^2)$. The structure was solved by direct methods and refined by alternate full-matrix least-squares cycles and difference Fourier maps. Hydrogen atoms were included at calculated positions but not refined. All non-hydrogen atoms were refined anisotropically. Bond distances (average Fe–Cl = 2.176 (10) Å for the two independent $FeCl_4^-$ in the asymmetric unit) and angles are normal for the $FeCl_4^-$ ion. Full tables of bond distances, angles, and positional and anisotropic displacement parameters and a listing of observed and calculated structure factors are available as supplementary material.

(29) Kovacic, P.; Brace, N. O. *J. Am. Chem. Soc.* **1954**, *76*, 5491.

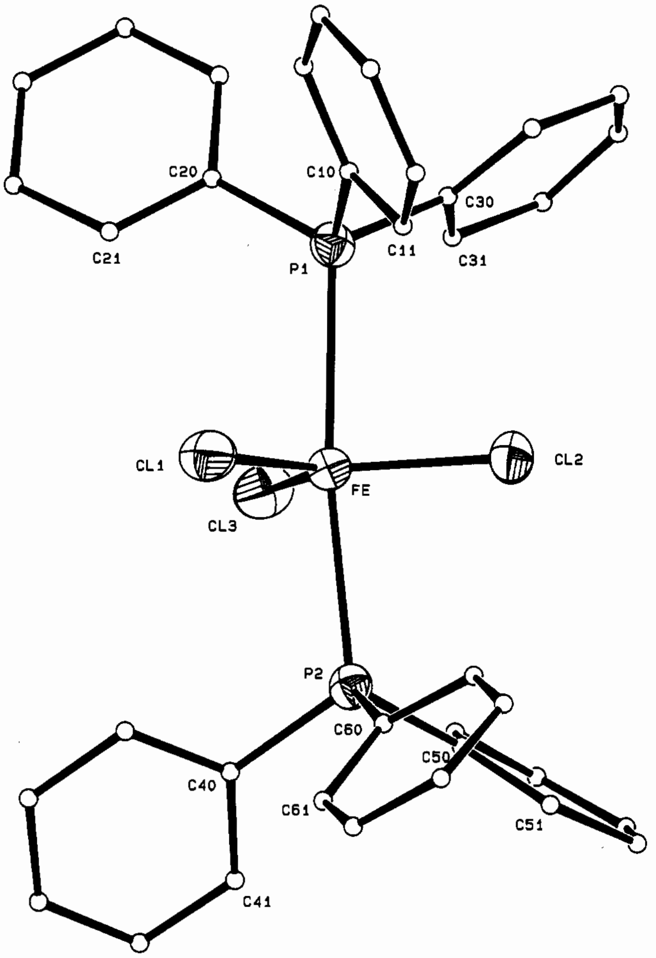

Figure 5. ORTEP view of the $FeCl_3(PPh_3)_2$ molecule with the atomic numbering scheme used. Carbon atoms are drawn with arbitrary radii, and hydrogen atoms are omitted for clarity.

nature *without* changing the oxidation state. The yellow oily material that we obtain probably represents the alternative decomposition product. It is tempting to suggest this product to correspond to the yellow $FeCl_3(PPh_3)$ reported by Singh and Rivest.[7] This oil was transformed into a crystalline solid by warming in the aromatic solvent under vigorous stirring. Unfortunately, however, this material is always contaminated by other products, such as $[PHPh_3][FeCl_4]$, deriving from the "reductive" decomposition pathway described above, and satisfactory analyses could not be obtained. We found that this yellow material readily dissolves in polar solvents such as MeCN and nitromethane, to give conductive solutions. On the basis of the formulation of this material as pure $[FeCl_2(PPh_3)_2][FeCl_4]$, we obtained a molar conductivity for a 10^{-3} M solution in nitromethane of 98.7 $mhos{\cdot}cm^2{\cdot}mol^{-1}$, well in the range reported[30] for 1:1 electrolytes.

The decomposition reaction in benzene gave the same products observed in toluene.

$FeCl_3(PMe_3)_2$ also decomposes if left in toluene solution for a long period of time. A white precipitate is obtained, and the violet solutions eventually become colorless. In analogy to the PPh_3 system, the decomposition reaction is retarded by an excess of the PMe_3 ligand. Unlike the case of $FeCl_3/PPh_3$ mixtures, we do not observe formation of oily material from $FeCl_3(PMe_3)_2$.

$FeCl_3(PCy_3)_2$ appears to be more stable in solution than its PPh_3 and PMe_3 counterparts. Unlike the PMe_3 adduct, which is very air sensitive, $FeCl_3(PCy_3)_2$ is air stable in the solid state for long periods of time.

2. In Halogenated Hydrocarbons. The decomposition of $FeCl_3(PPh_3)_2$ in halogenated hydrocarbons (CCl_4, $CHCl_3$, CH_2Cl_2) can be related to that observed in aromatic hydrocarbons.

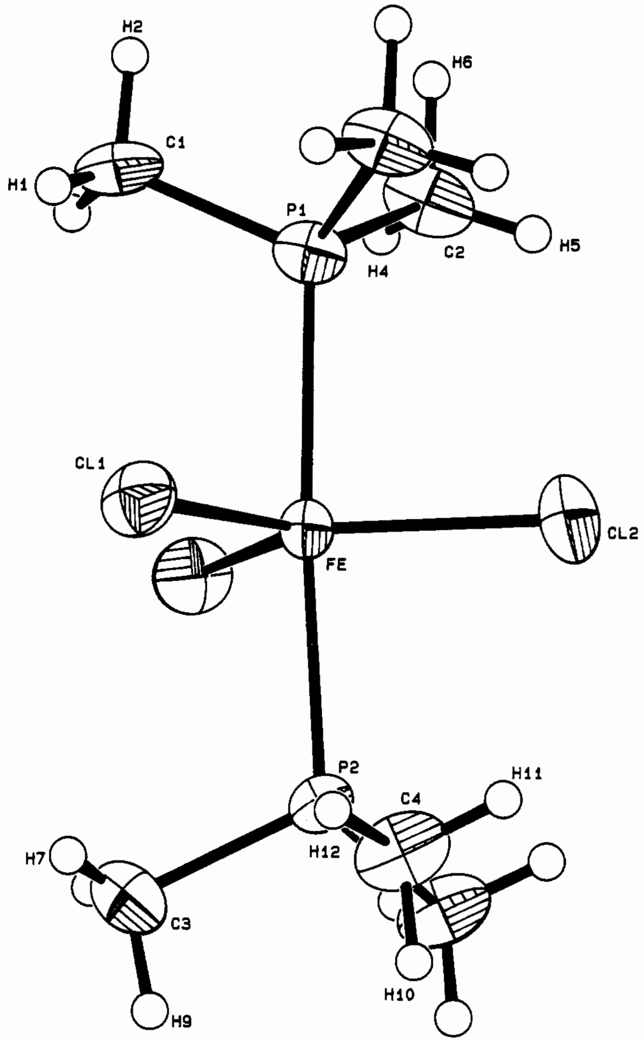

Figure 6. ORTEP view of the $FeCl_3(PMe_3)_2$ molecule with the atomic numbering scheme used. Hydrogen atoms are drawn with arbitrary radii for clarity.

In the proton-containing solvents, that is $CHCl_3$ and CH_2Cl_2, a white precipitate similar to the one that forms in toluene and benzene (see above) is obtained. This suggests reduction of the iron center at the expense of the solvent, which provides a proton for the formation of phosphonium salts. Gas-chromatographic analysis confirms this view: small amounts of CCl_4 (from $CHCl_3$) and $CHCl_3$ (from CH_2Cl_2) were detected. Once again, the amount of chlorinated solvent is less than expected on the basis of the reductive decomposition pathway. The remainder of $FeCl_3(PPh_3)_2$ probably converts to the same ionic isomer suggested above for the decomposition in toluene, which is soluble in chloroform and dichloromethane. We also have evidence for an additional decomposition pathway, involving attack of the phosphine ligand on the quaternary carbon of the solvent molecules. This type of reactivity is well documented in the literature[31] and can, in our case, be further encouraged by the Lewis acidity of the iron(III) center. This work has been published separately.[32]

In CCl_4, no reduction of Fe(III) to Fe(II) by action of the solvent is of course possible. However, decomposition of the $FeCl_3(PPh_3)_2$ solutions still occurs. The final mixture contains a brown oily material in a colorless solution. We have not further investigated the nature of this product.

---

(30) Geary, W. J. *Coord. Chem. Rev.* **1971**, *7*, 81.

(31) (a) Hantzsch, A.; Hibbert, H. *Chem. Ber.* **1907**, *40*, 1508. (b) Dehn, W. M.; Conner, R. B. *J. Am. Chem. Soc.* **1912**, *34*, 1409. (c) Ramirez, F.; McKelvie, N. *J. Am. Chem. Soc.* **1957**, *79*, 5829. (d) Driscoll, J. S.; Grisley, D. W., Jr.; Pustinger, J. V.; Harris, J. E.; Matthews, C. N. *J. Org. Chem.* **1964**, *29*, 2427. (e) Appel, R. *Inorg. Synth.* **1986**, *24*, 107. (f) Appel, R. *Inorg. Synth.* **1986**, *24*, 113.

(32) Walker, J. D.; Poli, R. *Polyhedron*, in press.

c. Crystallographic Studies. Both $FeCl_3(PPh_3)_2$ and $FeCl_3(PMe_3)_2$ crystallize in the orthorhombic system, the former with one molecule in the asymmetric unit and the latter with the molecule sitting on a crystallographically imposed mirror plane. Figures 5 and 6 show that both compounds have a mononuclear, trigonal-bipyramidal structure with the three chloro ligands in the equatorial plane and the two phosphine ligands in the axial positions. The 5-coordinate mononuclear, tbp structural arrangement around iron(III) has been proposed for a very limited number of compounds. Examples where the structure has been demonstrated by a X-ray crystallographic study are $[Fe(N_3)_5]^{2-}$,[33] $FeCl_3(4\text{-}NCC_5H_4N)_2$,[34] and $FeCl_3(NMe_3)_2$.[35] $\{FeCl_3dioxane\}_n$ has also been described as having an oligonuclear tbp structure,[36] whereas there is controversy about the $[FeCl_5]^{2-}$ ion.[37,38]

The Fe–Cl bond distances (see Tables IV and V) compare relatively well with those reported for the aforementioned tbp $FeCl_3L_2$ compounds [2.204 (1), 2.216 (1), and 2.229 (1) Å for L = $4\text{-}CNNC_5H_4$[34] and 2.207 (2) and 2.228 (1) Å for L = NMe_3[35]]. The most interesting feature of these structures are the Fe–P bond distances. In the PPh_3 compound, these are ca. 0.4 Å *longer* than the sum of Fe and P covalent radii (2.23 Å), whereas in the PMe_3 compound they are much closer to the expected value. Structures of other phosphine-containing Fe(III) compounds are, to the best of our knowledge, unavailable, so that a more significant comparison cannot be made. However, we observe that the distance between P and Fe(II) has also been found to vary over a wide range. Representative examples are 2.15–2.19 Å in $[MeC(CH_2PEt_2)_3Fe\{S_2C(PEt_2CH_2)_2CMe_2\}](BF_4)_2$,[39] 2.47 Å in $FeCl_2\{(i\text{-}Pr)_2PCH_2CH_2P(i\text{-}Pr)_2\}_2$,[40] 2.23–2.24 Å in $FeCl_2(Me_2PCH_2CH_2PMe_2)_2$,[41] and 2.66–2.71 Å in $FeCl_2\{Ph_2PCH_2CH_2P(Ph)CH_2CH_2PPh_2\}_2$.[41] These differences have been attributed to variations of the spin state, coordination number, steric effects, and electronic inductive properties of the phosphine ligands, listed in decreasing order of importance.[40,41]

In our case we have two molecules exhibiting the same geometry and coordination number. However, we have proven above that the two compounds have different magnetic properties, the PPh_3 compound being in a pure $S = {}^5/_2$ state and the PMe_3 compound having the larger contribution from the $S = {}^3/_2$ state. It is obvious that the phosphine ligand is held further away from the Fe center in the PPh_3 compound, where the d_{z^2} orbital (antibonding with respect to the Fe–P bond) contains one electron (see Figure 2). The Fe–P bond lengths in $FeCl_3(PPh_3)_2$, even in an absolute sense, appear extremely long. This can be attributed to the low affinity of the soft phosphine ligands toward hard metal centers. The paucity of Fe(III) compounds containing phosphine ligands is in agreement with this view.

Steric and inductive effects can, however, contribute to the observed bond length variation. The PPh_3 ligand, which shows a longer Fe–P bond with respect to PMe_3, is bulkier than the latter ligand. Steric effects have been previously invoked to explain the long Fe–N distances in the trigonal-bipyramidal Fe(III) complexes $FeCl_3L_2$ (L = $4\text{-}NCC_5H_4N$,[34] NMe_3[35]). The structural investigation of tbp Fe(III) complexes containing sterically demanding strong-field ligands (e.g. tricyclohexylphosphine) or less sterically demanding, weak donor ligands [e.g. $P(OCH_2)_3CCH_3$] might help sorting out the steric and electronic contributions to the Fe–P bond length. We have synthesized the PCy_3 derivative with this very objective in mind. We have proven that PCy_3 is a strong-field ligand, although not as strong as PMe_3 (vide supra), but unfortunately our attempts to obtain a crystal structure for the PCy_3 adduct have been so far thwarted by crystal twinning problems. Further studies in this field are in progress in our laboratory.

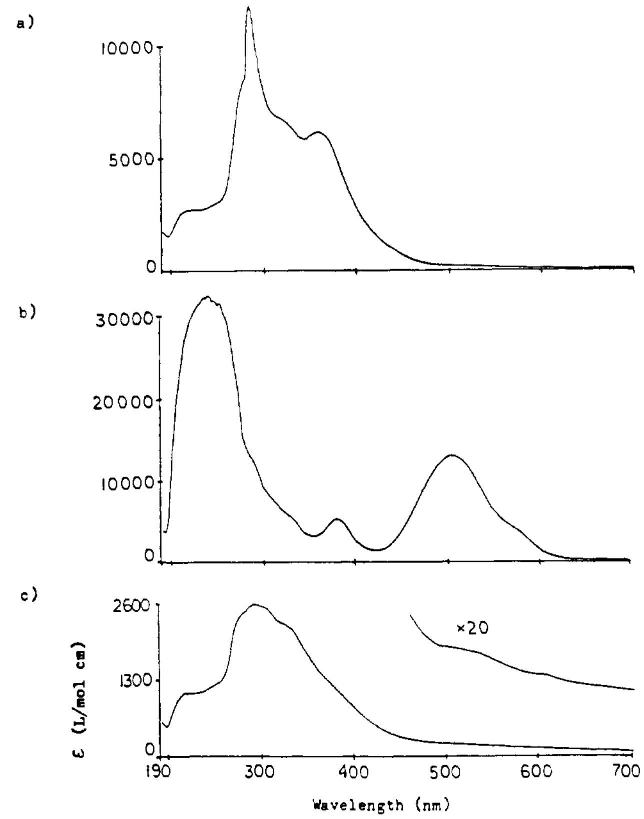

Figure 7. UV/visible spectra of $FeCl_3(PR_3)_2$ (toluene, room temperature): (a) R = Ph; (b) R = Me; (c) R = Cy.

d. Electronic Spectra. Additional evidence for the spin equilibrium between the $S = {}^5/_2$ and $S = {}^3/_2$ states for $FeCl_3(PR_3)_2$ compounds comes from the visible spectra. UV/visible spectra for the three compounds investigated in this work are reported in Figure 7.

Magnetic susceptibility data indicate that the $FeCl_3(PPh_3)_2$ compound is in a pure high-spin ($S = {}^5/_2$, ${}^6A_1'$) ground state, cf. Figure 2, column b. Since there are no spin-sextet excited states, no visible absorption band is expected. The lowest energy band is found in the UV region at 360 nm (see Figure 7a). For the PMe_3 compound, on the other hand, at least three bands are distinguishable in the visible and near-UV regions plus several others in the UV region (see Figure 7b). A trigonal-bipyramidal $S = {}^3/_2$ configuration (cf. Figure 4d) would have a ${}^4E''$ ground state and a number of accessible quartet excited states. These states can be derived from the splitting of the d^5 spectroscopic quartet terms (${}^4G$, ${}^4F$, ${}^4D$, ${}^4P$) by the D_{3h} ligand field (weak-field limit) or by action of the electronic correlation on the monoelectronic energy levels in a D_{3h} ligand field (strong-field limit). Taking the second approach, we would expect the following transitions: ${}^4E'' \rightarrow {}^4E'$ $[(e'')^3(e')^2 \rightarrow (e'')^2(e')^3]$; ${}^4E'' \rightarrow {}^4A_1''$, ${}^4E'' \rightarrow {}^4A_2''$, ${}^4E'' \rightarrow {}^4E''$ $[(e'')^3(e')^2 \rightarrow (e'')^3(e')^1(a_1')^1]$; ${}^4E'' \rightarrow {}^4A_1'$ (twice), ${}^4E'' \rightarrow {}^4A_2'$ (twice), ${}^4E'' \rightarrow {}^4E'$ (twice) $[(e'')^3(e')^2 \rightarrow (e'')^2(e')^2(a_1')^1]$. An assignment of the electronic transitions to the absorption bands is not trivial, and we leave it for interested experts. We simply observe that these absorption bands give supporting evidence for the presence of a $S = {}^3/_2$ spin state in solution. The PCy_3 compound is pale yellow-brown, and its magnetic properties are in agreement with the substantial population of the $S = {}^5/_2$ state at room temperature. In fact, the optical spectrum (Figure 7c) does not show strong absorptions in the visible region. However, contrary to the case for the PPh_3 adduct, weak visible bands can be observed. These bands may be assigned to optical transitions involving the slightly populated $S = {}^3/_2$ excited state.

It has to be noted that the ${}^4E''$ ground state of a d^5 configuration in a tbp geometry (Figure 2d) is degenerate and therefore subject

---

(33) Drummond, J.; Wood, J. S. *J. Chem. Soc., Chem. Commun.* **1969**, 1373.
(34) Daran, J.-C.; Jeannin, Y.; Martin, L. M. *Inorg. Chem.* **1980**, *19*, 2935.
(35) Millington, K. R.; Wade, S. R.; Willey, G. R.; Drew, M. G. B. *Inorg. Chim. Acta* **1984**, *89*, 185.
(36) Maeda, Y.; Takashima, Y. *Inorg. Nucl. Chem. Lett.* **1976**, *12*, 313.
(37) Creaser, C. S.; Creighton, J. A. *J. Inorg. Nucl. Chem.* **1979**, *41*, 469.
(38) Millikan, M. B.; James, B. D. *J. Inorg. Nucl. Chem.* **1981**, *43*, 1175.
(39) Bianchini, C.; Meli, A.; Orlandini, A.; Sacconi, L. *J. Organomet. Chem.* **1981**, *218*, 81.
(40) Hermes, A. R.; Girolami, G. S. *Inorg. Chem.* **1988**, *27*, 1775.
(41) Di Vaira, M.; Midollini, S.; Sacconi, L. *Inorg. Chem.* **1981**, *20*, 3430.

to Jahn–Teller distortion. A distortion of the axial bonds along the Berry psuedorotation coordinate would lower the symmetry to C_{2v} and generate the energy diagram shown in Figure 2, column e, for the iron 3d orbitals. The result is a net stabilization of the system and the distortion is therefore anticipated. Under such conditions, the absorption spectrum analysis may be even further complicated. We observe that the $FeCl_3(PR_3)_2$ (R = Ph, Me) structures *in the solid state* (see above) do not show a strong deviation of the P–Fe–P moiety from linearity [P(1)–Fe–P(2) = 172.4 (1)° for R = Ph, 176.3 (2)° for R = Me]. In fact, the structure of the PPh_3 compound, which is in a pure $S = {}^5/_2$ spin state and therefore not expected to give rise to Jahn–Teller distortion, appears more distorted than the structure of the PMe_3 compound. On the other hand, the Cl–Fe–Cl angles deviate more from the expected 120° value in the PMe_3 compound [115.1 (2) and twice 122.46 (9)° vs 122.6 (2), 118.3 (1), and 119.1 (2)° for the PPh_3 compound]. These small deviations are probably due to packing effects.

Acknowledgment. We are grateful to the University of Maryland, College Park (UMCP), MD, Chemistry Department, the UMCP General Research Board, the Camille and Henry Dreyfus Foundation (through a Distinguished New Faculty Award to R.P.), and the donors of the Petroleum Research Fund, administered by the American Chemical Society, for support. The X-ray diffractometer and MicroVax computer system were purchased in part with NSF funds (Grant CHE-84-02155). We thank Dr. L. Bennett and L. J. Swartzendruber for the SQUID solid-state variable-temperature magnetic studies on $FeCl_3(PMe_3)_2$ at the National Institute of Standards and Technology, Gaithersburg, MD. We also thank Profs. N. S. Dalal, B. M. Hoffman, and E. I. Solomon and one of the reviewers for helpful comments and Prof. H. Ammon for technical assistance with the X-ray diffractometer.

Supplementary Material Available: Full tables of crystal data, bond lengths, bond angles, and anisotropic displacement parameters for $FeCl_3(PPh_3)_2$, $FeCl_3(PMe_3)_2$, and $[PHPh_3][FeCl_4]$ and a table of positional parameters for $[PHPh_3][FeCl_4]$ (21 pages); listings of calculated and observed structure factors for $FeCl_3(PPh_3)_2$, $FeCl_3(PMe_3)_2$, and $[PHPh_3][FeCl_4]$ (73 pages). Ordering information is given on any current masthead page.

Contribution from the Department of Chemistry, University of Helsinki, Et. Hesperiankatu 4, 00100 Helsinki, Finland, and Department of Macromolecular Chemistry, Faculty of Science, Osaka University, Toyonaka, Osaka 560, Japan

REX Calculations. 12. Iteration Parameters for the 5f-Element Organometallics of Thorium–Neptunium. Geometries of ThO_2 and UO_2^{2+} Revisited

Pekka Pyykkö,*[†] Liisa J. Laakkonen,[†] and Kazuyuki Tatsumi*[‡,§]

Received July 29, 1988

Iterative relativistic extended Hückel (REX) energy parameters giving realistic metal orbital populations for organometallic compounds are presented for the early actinoids, An = Th–Np. The energy levels for $An(C_8H_8)_2$ are also reasonable. A transition from 5fδ toward $5f_{5/2}$ bonding is noticed in the actinocene series. The problem "Why is uranyl linear while the isoelectronic ThO_2 is bent?" is revisited within the REX model.

1. Introduction

The object of the present work is to see whether a realistic description of the electronic structure of the organometallic compounds of the early actinoids (Th–Np) is possible at the crudest semiempirical level, viz. the extended Hückel (EH) one. Our relativistic extended Hückel method (REX) contains the radial and energetic relativistic effects, including spin-orbit splitting, but its earliest applications on actinoid systems[1] were noniterative and led to an exaggerated ionicity.

One can outline three philosophies for EH calculations.[2] (1) "Organic" with the traditional Hoffmann parameters, no iterations, and no Madelung corrections; (2) "organometallic" with the traditional ligand parameters and iterations for the metal atoms only, without Madelung corrections; (3) "inorganic" in which all atoms are iterated, with the Madelung corrections. Simulating the Hartree-Fock method, this method gives decent MOs and orbital energies but no well-defined total energy. For recent reviews, see ref 2 and 3. In cases 1 and 2, a reasonable description of all properties (atomic populations of the MOs, relative orbital energies, and total energies) is attempted.

Charge iterations were added to REX following method 3 in ref 4. We now consider philosophy 2 for REX using the metal characters and orbital energies from earlier scattered wave,[5-7] relativistic HFS,[8] and pseudopotential HF[9] data on the actinocenes, $An(COT)_2$ (COT = C_8H_8), or cyclopentadienyls, $An(cp)_4$ (cp = C_5H_5), as reference points.

We also report quasirelativistic (QR), one-component averages of the present radial and energetic parameters. They can be used in traditional EH programs and contain the other relativistic effects, apart from spin–orbit splittings. Applications have already been published.[10,11]

Finally we return to the issue "Why is uranyl linear and the isoelectronic ThO_2 bent?"[1,4,12-14] An aspect not fully considered before is the influence of the bond length.

[†] University of Helsinki.

[‡] Work performed at the University of Helsinki under a scholarship from the Neste Oy Foundation.

[§] Osaka University.

(1) Pyykkö, P.; Lohr, L. L., Jr. *Inorg. Chem.* **1981**, *20*, 1950.

(2) Pyykkö, P. In *Methods in Computational Chemistry*; Wilson, S., Ed.; Plenum Press: London and New York, 1988; Vol. 2. This review also contains a diskette with the ITEREX program for an IBM PC.

(3) Albright, T. A.; Burdett, J. K.; Whangbo, M.-H. *Orbital Interactions in Chemistry*; Wiley: New York, 1985.

(4) Larsson, S.; Pyykkö, P. *Chem. Phys.* **1986**, *101*, 355.

(5) Rösch, N.; Streitweiser, A., Jr. *J. Am. Chem. Soc.* **1983**, *105*, 7237.

(6) Rösch, N. *Inorg. Chim. Acta* **1984**, *94*, 297.

(7) Bursten, B. E.; Casarin, M.; di Bella, S.; Fang, A.; Fragalà, I. L. *Inorg. Chem.* **1985**, *24*, 2169.

(8) (a) Boerrigter, P. M. Spectroscopy and Bonding of Heavy Element Compounds. Thesis, Vrije Universiteit: Amsterdam, 1987. (b) Boerrigter, P. M.; Baerends, E. J.; Snijders, J. G. *Chem. Phys.* **1988**, *122*, 357.

(9) Chang, A. H. H.; Pitzer, R. M. Submitted for publication.

(10) Tatsumi, K.; Nakamura, A. *Organometallics* **1987**, *6*, 427.

(11) Tatsumi, K.; Nakamura, A. *J. Am. Chem. Soc.* **1987**, *109*, 3195.

(12) Tatsumi, K.; Hoffmann, R. *Inorg. Chem.* **1980**, *19*, 2656.

(13) Wadt, W. R. *J. Am. Chem. Soc.* **1981**, *103*, 6053.

(14) Pyykkö, P.; Laaksonen, L. *J. Phys. Chem.* **1984**, *88*, 4892.

0020-1669/89/1328-1801$01.50/0 © 1989 American Chemical Society